Synthesis, Structure, and Redox Chemistry of Ethenyl and Ethynyl Ferrocene Polyaromatic Dyads

Laurence Cuffe,[†] Richard D. A. Hudson,[†] John F. Gallagher,[†] Sarah Jennings,[†] C. John McAdam,[‡] Rosamond B. T. Connelly,[‡] Anthony R. Manning,[†] Brian. H. Robinson,*[,‡] and Jim Simpson[‡]

Department of Chemistry, University College Dublin, Belfield, Dublin 4, Ireland, and Department of Chemistry, University of Otago, PO Box 56, Dunedin, New Zealand

Received September 21, 2004

A series of ferrocenyl−arene dyads, Fc−C≡C−Ar, *trans*-Fc−CH=CH−Ar, and Fc−CH=CH−CH=CH−Ar (Ar = phenyl, 1-naphthyl, 2-naphthyl, 9-phenanthryl, 9-anthryl, 1-pyrenyl, 3-perylenyl) have been synthesized. Their structures and spectroelectrochemical properties are discussed. The molecular structures of several have been determined by X-ray diffraction and the observed structures compared with global free-energy minimized calculated structures. In the solid state all ethynyl dyads have the aromatic ring orthogonal to the ferrocenyl cyclopentadienyl rings, whereas calculations predict a coplanar orientation. Calculated and observed structures agree for the ethenyl dyads with the rings orthogonal and coplanar for the anthryl and pyrenyl dyads, respectively. In most cases the solid-state structures are stabilized by offset π-stacking interactions between the polycyclic hydrocarbon rings. The two bands in the electronic spectra of the neutral dyads are due to the individual aryl and ferrocenyl end-groups. Upon oxidation at the $[Fc]^{+/0}$ couple, the ferrocenyl transition is replaced by LMCT bands at lower energy and a new weak band in the NIR assigned to a $Fc^+ \leftarrow$ aryl transition; these assignments are supported by resonance Raman spectra, and the energy of the $Fc^+ \leftarrow$ aryl transition correlates with the ionization energy of the aryl group. These are therefore electrochromic dyads.

Introduction

Ferrocenyl derivatives fulfill many of the broad criteria for the development of molecular materials for specific technological application.[1] In particular, donor−acceptor assemblages incorporating the ferrocenyl group as a donor have been the subjects of considerable recent research, as their attractive electronic and physical properties make them suitable candidates for NLO materials,[2−5] electrode surface modifiers,[6] and magnetic surface materials.[7] Structure−property relationships for derivatives of electron-rich ferrocenyl and alkylferrocenyl groups linked to electron acceptors (including metal-centered acceptors) are well established.[2,3] In these compounds charge separation may become important as the acceptor strength increases, but in most cases the LUMO is centered on the acceptor with some delocalization onto the unsaturated link. Many examples are based on ferrocenyl-substituted arylethenes or arylethenyl oligomers (aryl = phenyl, thiophenyl), yet surprisingly few reports describe the chemistry of larger aromatic analogues.[8,9]

The ferrocenyl−ferrocenium redox couple adds a further dimension to an investigation of these donor−acceptor compounds. Ferrocenyl [Fe(II)]−ferrocenium [Fe(III)] mixed-valence species, formed when diferrocenyl systems are partially oxidized, have been extensively studied,[10] and many display classical Class II donor−acceptor behavior. In contrast, donor−acceptor chemistry where the ferrocenium cation is potentially the acceptor to a non-ferrocenyl donor has been reported[4,11]

* To whom correspondence should be addressed. E-mail: anthony.manning@ucd.ie; brobinson@alkali.otago.ac.nz.
† University College Dublin.
‡ University of Otago.

(1) Marder, S. R. *Inorganic Materials*, 2nd ed.; Bruce, D. W., O'Hare, D., Eds.; Wiley: Chichester, 1996. (b) Long N. J. *Angew. Chem., Int. Ed. Engl*. **1995**, *34*, 21. (c) Hudson, R. D. A. *J. Organomet. Chem.* **2001**, *637−639*, 47.

(2) (a) Barlow, S.; Bunting, H. E.; Ringham, C.; Green, J. C.; Bublitz, G. U.; Boxer, S. G.; Perry, J. W.; Marder, S. R. *J Am Chem Soc.* **1999**, *121*, 3715. (b) Barlow S. *Inorg. Chem*. **2001**, *40*, 7047.

(3) Barlow, S.; Marder, S. R. *Chem. Commun.* **2000**, 1555.

(4) Malaun, M.; Kowallick, R.; McDonagh, A. M.; Marcaccio, M.; Paul, R. L.; Asselberghs, I.; Clays, K.; Persoons, A.; Bildstein, B.; Fiorini, C.; Nunzi, J.-M.; Ward, M. D.; McCleverty, J. A. *J. Chem. Soc., Dalton Trans*. **2001**, 3025.

(5) (a) Asiri, A. M. *Appl. Organomet. Chem.* **2001**, *15*, 907. (b) Stankovic, E.; Toma, S.; Boxel, R. V.; Asselberghs, I.; Persoons, A. *J. Organomet. Chem.* **2001**, *637−639*, 426, and references therein. (c) Li, G.; Song, Y.; Hou, H.; Li, L.; Fan, Y.; Zhu, Y.; Meng, X.; Mi, L. *Inorg. Chem.* **2003**, *42*, 913. (d) Shin, D. M.; Lee, I. S.; Chung, Y. K. *Eur. J. Inorg. Chem.* **2003**, 2311. (e) Mata, J. A.; Peris, E.; Uriel, S.; Llusar, R.; Asselberghs, I.; Persoons, A. *Polyhedron* **2001**, *20*, 2083.

(6) Armstrong, N. R.; Carter, C.; Donley, C.; Simmonds, A.; Lee, P.; Brumbach, M.; Kippelen, B.; Domercq, B.; Yoo, S. *Thin Solid Films* **2003**, *445*, 342. (b) Zou, C.; Wrighton, M. S. *J. Am. Chem. Soc.* **1990**, *1I2*, 7578.

(7) Miller, J. S.; Epstein, A. J. *Angew. Chem., Int. Ed. Engl.* **1994**, *33*, 385.

(8) McKinney, J. D.; Anderson, P. A.; Hamor, T. A.; Jones, C. J.; Paxton, K.; Porch, A. *J. Organomet. Chem*. **1998**, *558*, 147.

(9) (a) Liu, S. G.; Perez, I.; Martin, N.; Echegoyen, L. E. *J. Org. Chem.* **2000**, *65*, 9092. (b) Butler, I. R.; Callabero, A. G.; Kelly, G. A.; Amey, J. R.; Kraemer, T.; Thomas, D. A.; Light, M. E.; Gelbrich, T.; Coles, S. J. *Tetrahedron Lett.* **2004**, *45*, 467.

(10) Ribou, A.-C.; Launay, J.-P.; Sachtleben, M. L.; Li, H.; Spangler, C. W. *Inorg. Chem.* **1996**, *35*, 3735.

(11) Mendiratta, A.; Barlow S.; Day, M. W.; Marder S. R. *Organometallics* **1999**, *18*, 454.

10.1021/om0492653 CCC: $30.25
Publication on Web 03/19/2005

but not explored to any extent. Of interest to us is the possibility of modulating the emission characteristics of fluorophores using the different quenching characteristics of the ferrocenyl group and the ferrocenium cation. Both energy and electron transfer may be involved in quenching processes, depending on the nature of the excited species.[12] Recent work from this laboratory has provided examples of both enhanced and reduced emission upon oxidation of the ferrocenyl moiety.[13−15] If reversible, this feature provides an on−off fluorescent switch capability. To date, we have concentrated on fluorophores that were good electron acceptors in the ground state (naphthalimides, acridones, acridines). The work reported in this paper was carried out in order to extend ferrocenyl dyad chemistry to those where the non-ferrocenyl component was a donor. Donor end-groups were required that would have orbitals of suitable configurations and energies to allow them to communicate via a conjugated π-linkage to both the ferrocenyl (Fc) and ferrocenium (Fc^+) moieties. It was also recognized that intermolecular as well as intramolecular interactions can perturb ground and excited states where the donor has aromatic functionality; for example, π-stacking was a feature of the structural and spectroelectrochemistry of Fc-π-linked-naphthalimide dyads.[15] A set of donors that fulfilled these criteria were the polycyclic aromatic hydrocarbons. Those selected (1- and 2-naphthyl, phenanthryl, anthryl, pyrenyl, and perylenyl) have a range of oxidation potentials more positive than ferrocene and the ability to π-stack. Herein, we describe the synthesis and structural and spectroelectrochemical features of the neutral precursors, Fc−C≡C−Ar, Fc−CH═CH−Ar, and Fc−CH═CH−CH═CH−Ar, and the spectroscopic properties of the ferrocenium dyads derived from them. The calculated orbital configurations, a detailed analysis of the low-energy electronic spectra for ferrocenyl−arene and related dyads, and emission behavior are reported elsewhere.[16]

Results and Discussion

The ferrocenyl arylethynes (Fc−C≡C−Ar) were prepared by Sonogashira coupling of ethynylferrocene with the respective arylbromide [R = 1-naphthyl (**2**),[17] 2-naphthyl (**3**), 9-phenanthryl (**4**), 9-anthryl (**5**)] or aryliodide [R = 1-pyrenyl (**6**), 3-perylenyl (**7**)] in boiling $^iPr_2NH$ (Scheme 1). Fc−C≡C−phenyl (**1**)[18] was prepared using similar conditions by the coupling of FcI with ethynylbenzene. Interestingly, similar attempts to prepare **6** from 1-ethynylpyrene and FcI were unsuccessful.

The ferrocenyl arylethenes **8**−**12**, **13**,[8] and **14** were prepared by Wittig reaction of ferrocenylmethyl triphenylphosphonium iodide with the respective aryl aldehyde (Scheme 1). Both diastereomers were obtained from the reactions, but no attempt was made to separate them. They were converted to the *E* form by refluxing with molecular iodine in CH_2Cl_2 solution. The accepted mechanism for cis−trans isomerization in organic substrates is shown in Scheme 2a, but for ferrocenyl alkenes a mechanism via a fulvene intermediate of a ferrocenium species could be considered (Scheme 2b). **8** and **10** have been prepared previously[19] by the SmI_2-promoted reaction of FcCHO with $ArCH_2Br$ and by the cross-metathesis of $ArCH{=}CH_2$ with Fc−CH═CH_2.[20] **8**, **13**, and **15** have been prepared previously from FcCHO with the Wittig reagent derived from the appropriate ferrocenyl or aryl triphenylphosphonium salt.[8,21]

Scheme 1. Preparation of Ethynyl and Ethenyl Compounds

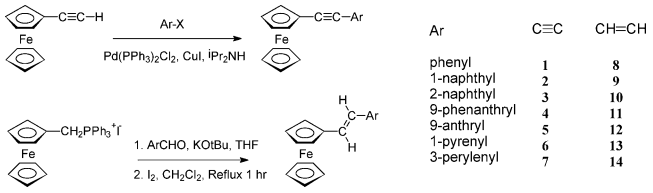

Ar	C≡C	CH=CH
phenyl	1	8
1-naphthyl	2	9
2-naphthyl	3	10
9-phenanthryl	4	11
9-anthryl	5	12
1-pyrenyl	6	13
3-perylenyl	7	14

Scheme 2. Mechanism for Isomerization

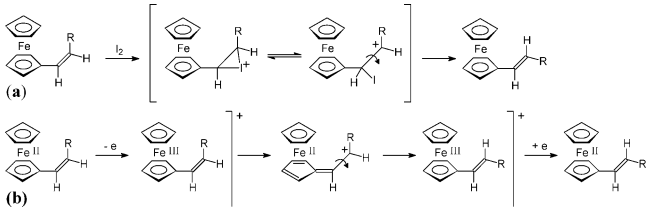

Scheme 3. Preparation of Dienes

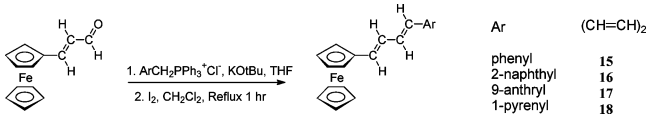

Ar	$(CH{=}CH)_2$
phenyl	15
2-naphthyl	16
9-anthryl	17
1-pyrenyl	18

The dienes **15**−**18** were prepared from Fc−CH═CH−CHO[22] and the appropriate arylmethylphosphonium salt (Scheme 3). This reaction generated a mixture of various isomers that were converted to the *E*,*E*-isomer by refluxing with a crystal of iodine.

1−**18** were orange to red-orange crystalline solids, with the exception of **4**, which was obtained as a red-orange oil. They were soluble in a range of common organic solvents, polar and nonpolar, but particularly dichloromethane. The degree of solubility decreased with the size of the polyaromatic. All compounds were characterized by microanalysis, mass spectra, and NMR and IR spectroscopy. The IR spectra are generally unremarkable, but when Ar = phenyl, 1- and 2-naphthyl, and pyrenyl (**1**−**3**, **6**), the $\nu_{C\equiv C}$ band is split in both solution and solid-state (KBr) spectra, an effect perhaps attributable to Fermi coupling.[23] This splitting has also

(12) Fery-Forgues, S.; Delavaux-Nicot, B. *J. Photochem. Photobiol. A* **2000**, *132*, 137, and references therein.
(13) McGale, E. M.; Robinson. B. H.; Simpson, J. *Organometallics* **2003**, *22*, 931.
(14) McAdam, C. J.; Robinson, B. H.; Simpson, J. *Organometallics* **2000**, *19*, 3644.
(15) McAdam, C. J.; Morgan, J. L.; Robinson, B. H.; Simpson, J. *Organometallics* **2003**, *22*, 5126.
(16) Flood, A.; Gordon, K.; Kjaergaard, H.; Manning, A. M.; McAdam, C. J.; Robinson, B. H.; Simpson, J. *Dalton*, submitted for publication.
(17) Rausch, M. D.; Siegel, A. *J. Org. Chem.* **1969**, *34*, 1974.
(18) Rausch, M. D.; Siegel, A.; Klemann, L. P. *J. Org. Chem.* **1966**, *31*, 2703.
(19) Jong, S.-J.; Fang, J.-M. *J. Org. Chem.* **2001**, *66*, 3533.
(20) (a) Yasuda, T.; Abe, J.; Iyoda, T.; Kawai, T. *Chem. Lett.* **2001**, 812. (b) Yasuda, T.; Abe, J.; Yoshida, H.; Iyoda, T.; Kawai, T. *Adv. Synth. Catal.* **2002**, *344*, 705.
(21) (a) Pauson, P. L.; Watts, W. E. *J. Chem. Soc.* **1963**, 2990. (b) Drefahl, G.; Plotner, G.; Winnefeld, I. *Ber.* **1962**, *95*, 2788.
(22) Spangler, C. W.; McCoy, R. K. *Synth. Commun.* **1988**, *18*, 51.
(23) Paul, F.; Mevellec, J.-Y.; Lapinte, C. *J. Chem. Soc., Dalton Trans.* **2002**, 1783.

Table 1. Selected ^{13}C NMR, Electrochemical, and Spectral Data

	H	phenyl	1-naphth.	2-naphth.	phenan.	anthryl	pyrenyl	peryl.
^{13}C NMR[a]								
Fc−*C*≡C	82.7	88.4	93.5	88.8	93.2	100.1	94.4	94.8
C≡*C*−R	73.6	85.8	83.9	86.2	84.1	82.6	85.0	84.4
Fc−*C*=C	134.7	127.0	130.0	127.5	130.5	135.6	130.4	130.1
C=*C*−R	111.1	126.1	123.0	126.2	123.5	121.9	123.0	122.8
E[Fc]$^{+/0}$[b]								
Fc−C≡C	0.72	0.67	0.68	0.67	0.67	0.67	0.67	0.67
Fc−C=C	0.56	0.55	0.55	0.54	0.56	0.59	0.55	0.55
λ_{max}								
B(Fc−C≡C)[c]	443	446	446	446	446	*d*	446	*d*
B (Fc−C=C)[c]	446	456	456	458	457	*d*	457	*d*
B′(Fc−C≡C)[e]		420	403−524	400−464	410−484	412−476	458−570 625	505[e]
B″		575	583	580	587	711		810
B′(Fc−C=C)[e]		401−475	384−500	420−492	382−500	380−472	471−570 650	530[e]
B″		585	590		590	700		800
C(Fc−C≡C)[f]		797	873	850	898	1120	1020	1210
C(Fc−C=C)[f]		900	956	959	955	1050	1110	1310

[a] In $CDCl_3$. [b] In CH_2Cl_2, Pt, 0.1 M $TBAPF_6$ at 20 °C. [c] In CH_2Cl_2; λ nm range for structured band **B′**. [d] Obscured by aryl transition. [e] Electrochemically generated ferrocenium species, CH_2Cl_2, λ nm. [f] ϵ for **C** increases from Ph 0.7 to pyrenyl 1.6 (mol^{-1} cm^{-1} L × 10^{-3}).

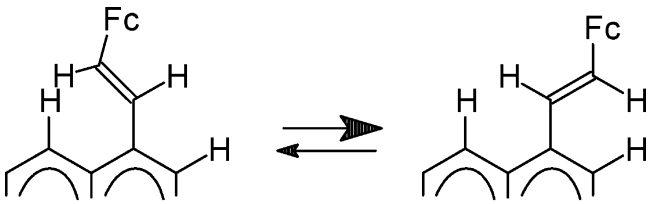

Figure 1. Steric interaction in ethenyl PAH derivatives.

been observed for other ferrocenyl alkynes[24a] and in 1,1″-bis(arylethynyl)biferrocenes,[24b] where $\nu_{C\equiv C}$ is split when Ar = phenyl, 1-naphthyl, and pyrenyl compounds, but not anthryl.

Complete assignments of ^{1}H and ^{13}C NMR resonances were made using homonuclear (COSY, NOESY, and TOCSY) and heteronuclear (DEPT, HSQC, and CIGAR) methods. Selected ^{13}C data are given in Table 1; full ^{1}H and ^{13}C NMR assignments are given in the Supporting Information. The three ferrocene resonances (H_α, H_β, and C_5H_5) in the ^{1}H NMR showed a small progression to lower field with increasing size of the aryl group in both the ethene and ethyne series. The assignment of ferrocenyl H_α to low field of H_β for Fc−C≡C−Ar follows a study of 2,5-dideutero derivatives of ethynylferrocene and Fc−C≡C−phenyl.[25] An assignment of H_α protons to low field of H_β for Fc−CH=CH−Ar was confirmed by NOE and CIGAR correlations and agrees with that for vinylferrocene.[25] Our assignment of the alkene protons (Fc−C*H*= and =C*H*−Ar) from NOE is consistent with those of ethenylarenes[26] and backed up by CIGAR correlations. The NOEs reflect a conformational preference (seen also in the solid-state structures) that where possible avoids "fjord" type interactions[27] between proximal hydrogens. For **13**, the calculated difference in energy between the configuration with minimium proximal interactions (Figure 1b) and that in which the ferrocenyl-C*H*= is closest to the proximal pyrene hydrogen (Figure 1a) is calculated to be 6.02 kJ/mol. All the ethenyl aryls are able to adopt this sterically less hindered conformation that allows ethenyl and aryl coplanarity. The exception is the ethenylanthryl dyad **12**, where an unusually low Fc−C*H*= shift of 6.71 (Table 1) suggests that coplanarity is not maintained (as in the solid state, vide infra). Anomalous behavior associated with this particular dyad will be noted consistently throughout this paper.

A J_{HH} coupling constant of 16 Hz confirmed the *trans*-(*E*)-conformation of the ethene compounds. Chemical shifts for the ferrocenyl and aryl components in the butadienyl compounds **15**−**18** closely resembled their ethenyl counterparts. The alkenyl protons showed the appropriate coupling (doublet 15 Hz, *H1* and *-4*; dd 15, 11 Hz, *H2* and *-3*) for an *E*,*E*-configuration, and this order of connectivity was confirmed by TOCSY measurements.

^{13}C NMR spectra of the Fc−C≡C−Ar, **1**−**7**, and Fc−CH=CH−Ar, **8**−**14**, compounds resembled their respective ferrocenyl precursors, Fc−C≡C−H and Fc−CH=CH_2; the Ar component of **8**−**14**, that of the respective vinyl arene.[26] ^{13}C chemical shifts of the four ferrocenyl carbon signals (*ipso*, α, *β*, and Cp) were more dependent on the *π*-linker than the Ar group (Table S1). HSQC, supported by $^4J_{CH}$ CIGAR correlations, showed the ferrocenyl C_α resonance is low field of C_β for the ethyne series but reversed in the ethene series. There is some confusion in the literature[24,28] on this point. Assignment of the alkyne carbon resonances was based on a consistent $^3J_{CH}$ correlation (CIGAR) of an ortho-aryl proton to one of the ethyne ^{13}C resonances, and assignment of the ethene ^{13}C resonances was unambiguous from HSQC. Subtle variations occur with Ar so that for *δ*(Fc−*C*≡C) and *δ*(Fc−*C*H=CH), the lowest chemical shifts were observed for Ar = Ph (**1** and **8**) or 2-naphthyl, and the highest for 9-anthryl (**5** and **12**), whereas for *δ*(C≡*C*−Ar) and *δ*(CH=*C*H−Ar) the trend is reversed and shifts decreased in the series from **1** → **7** and **8** → **14**.

Structural Analysis. Structures and atom-numbering schemes for the alkyne complexes **5**, **6**, and **7** are

(24) (a) Stepnicka, P.; Trojan, L.; Kubista, J.; Ludvik, J. *J. Organomet. Chem.* **2001**, *637*−*639*, 291. (b) McAdam, C. J. Unpublished work.

(25) Rausch, M. D.; Siegel, A. *J. Organomet. Chem.* **1969**, *17*, 117.

(26) Katritzky, A. R.; Hitchings, G. J.; King, R. W.; Zhu, D. W. *Magn, Reson, Chem.* **1991**, *29*, 2.

(27) Bartle, K. D.; Jones, D. W. *Adv. Org. Chem.* **1972**, *8*, 317.

(28) (a) Koridze, A. A.; Petrovskii, P. V.; Mokhov, A. I.; Lutsenko, A. I. *J. Organomet. Chem.* **1977**, *136*, 57. (b) Pickett, T. E.; Richards, C. J. *Tetrahedron Lett.* **1999**, *40*, 5251. (c) Yuan, Z.; Stringer, G.; Jobe, I. R.; Kreller, D.; Scott, K.; Koch, L.; Taylor, N. J.; Marder, T. B. *J. Organomet. Chem.* **1993**, *452*, 115.

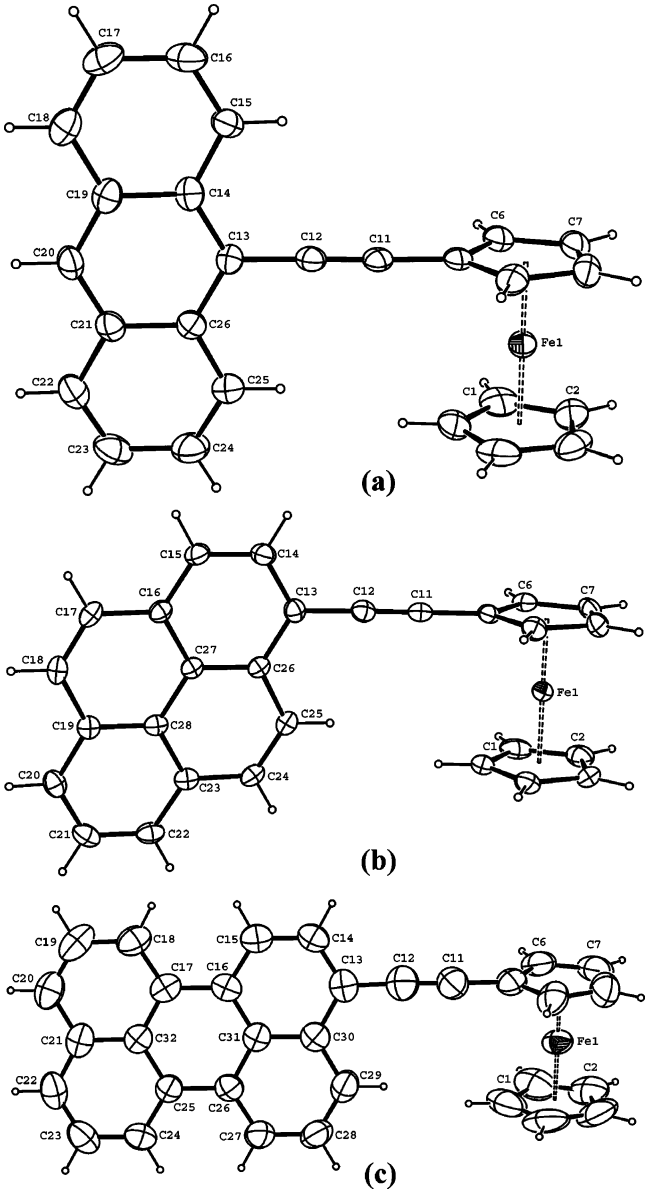

Figure 2. Perspective views of the ethynyl dyads, (a) **5**, (b) **6**, and (c) **7**, showing the atom-numbering schemes. For clarity only the first two C atoms of the consecutively numbered cyclopentadienyl rings have been labeled.

shown in Figure 2a−c, and those of the alkene systems **12** and **13** in Figure 3a,b. Selected bond length and angle data for all compounds are given in Table 2, with packing information in Table 3.

The structures of **5**, **6**, and **7** comprise an alkyne unit C(11)≡C(12) substituted with a ferrocenyl group at C(11) and the polyaromatic hydrocarbon at C(12). **5** has an anthracene residue substituted in the 9-position, **6** a 1-substituted pyrene, and **7** a 3-substituted perylene moiety. The C(11)≡C(12) distances are unremarkable and do not vary significantly with the nature of the hydrocarbon substituent. The cyclopentadienyl rings of each of the ferrocene residues are approximately eclipsed, with interplanar angles of 0.83(12)° for **5**, 0.61(19)° for **6**, and 1.4(5)° for **7**.

Structures of the alkene complexes **12** and **13** confirm *E*-configurations of the ferrocenyl and hydrocarbon substituents on the C(11) and C(12) atoms of the alkene units. There are small but significant differences between the two alkene moieties. The C(11)=C(12) bond in **13** is longer (1.339(4) Å) and the C(12)−C(13) distance, 1.466(4) Å, shorter than the corresponding vectors for **12**, 1.323(3) and 1.484(3) Å respectively. However, it is not possible to determine whether these differences result from steric or electronic effects. The cyclopentadienyl rings in both ferrocene moieties are again eclipsed, with interplanar angles of 1.8(6)° for **12** and 1.9(3)° for **13**. The structures of **8** and **10** have also been reported,[20] but unfortunately no metrical details are currently available to allow comparison with the structures reported here. However the molecular structure figures suggest that for both their C_5H_4, CH=CH, and aromatic groups lie close to the same plane as found for **13**, rather than the situation found in **12**, where the aromatic group lies approximately perpendicular to that plane.

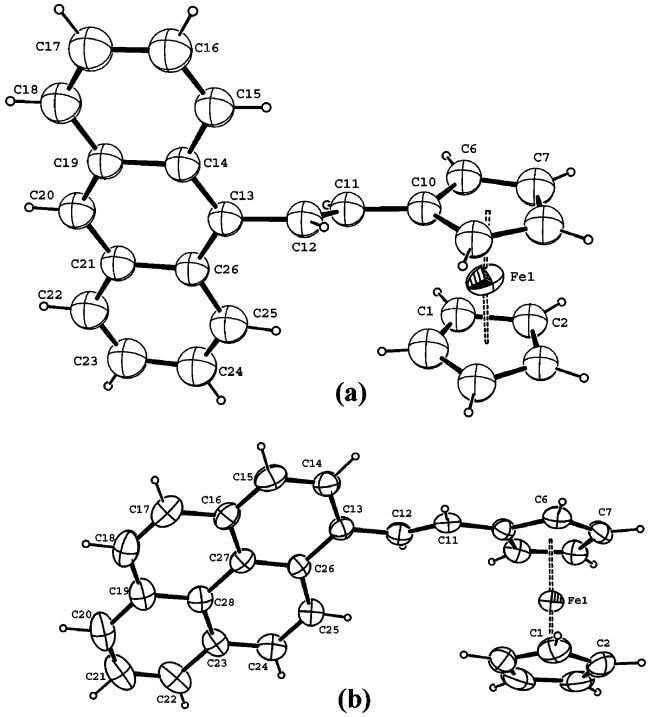

Figure 3. Perspective views of the ethenyl dyads (a) **12** and (b) **13** showing the atom-numbering schemes. For clarity only the first two C atoms of the consecutively numbered cyclopentadienyl rings have been labeled.

An important question in this series of dyads is the relative orientation of the ferrocenyl and polyaromatic rings. Knowledge of this detail is important in the interpretation of the spectroscopic and redox data. Therefore the X-ray structures of **5**−**7**, **12**, and **13** were compared with those predicted from B3LYP calculations of the energy-minimized structures. In all of the alkyne derivatives **5**−**7**, the cyclopentadienyl and polyaromatic rings are essentially *orthogonal* in the solid state, whereas the calculated minimized structures predict them to be coplanar. In contrast, there is good agreement between the calculated minimized structure and the solid-state structure for the ethenylanthracene derivative **12**. Here the free global minimum was found to occupy a geometry in which the substituted cyclopentadienyl ring is almost *perpendicular* to the plane

Table 2. Selected Bond Lengths (Å) and Angles (deg) for 5−7, 12, and 13

	5	6	7	12	13
C(10)−C(11)	1.434(4)	1.440(3)	1.437(8)	1.456(3)	1.447(4)
C(11)−C(12)	1.192(4)	1.195(3)	1.221(8)	1.323(3)	1.339(4)
C(12)−C(13)	1.439(4)	1.444(3)	1.425(8)	1.484(3)	1.466(4)
C(13)−C(14)	1.411(5)	1.404(3)	1.376(7)	1.411(2)	1.407(4)
C(13)−C(26)	1.421(5)	1.427(3)		1.411(3)	1.413(3)
C(13)−C(30)			1.434(7)		
C(14)−C(15)	1.425(5)	1.379(3)	1.377(7)	1.429(3)	1.378(4)
C(14)−C(19)	1.433(4)			1.433(3)	
C(15)−C(16)	1.354(5)	1.409(3)	1.400(7)	1.357(3)	1.391(4)
C(16)−C(17)	1.417(5)	1.443(3)	1.477(7)	1.408(3)	1.430(4)
C(16)−C(27)		1.427(3)			1.429(4)
C(16)−C(31)			1.417(6)		
C(17)−C(18)	1.363(5)	1.346(3)	1.381(7)	1.351(3)	1.345(4)
C(17)−C(32)			1.424(7)		
C(18)−C(19)	1.427(5)	1.443(3)	1.389(9)	1.427(3)	1.442(4)
C(19)−C(20)	1.395(5)	1.398(3)	1.351(9)	1.392(3)	1.399(4)
C(19)−C(28)		1.425(3)			1.416(4)
C(20)−C(21)	1.395(5)	1.399(4)	1.426(8)	1.388(3)	1.390(4)
C(21)−C(22)	1.429(5)	1.376(4)	1.412(8)	1.430(3)	1.376(4)
C(21)−C(26)	1.439(4)			1.436(3)	
C(21)−C(32)			1.427(7)		
C(22)−C(23)	1.345(5)	1.416(3)	1.357(8)	1.345(3)	1.398(4)
C(23)−C(24)	1.413(5)	1.437(3)	1.404(8)	1.411(4)	1.421(4)
C(23)−C(28)		1.424(3)			1.431(4)
C(24)−C(25)	1.354(5)	1.359(3)	1.391(7)	1.363(3)	1.354(4)
C(25)−C(26)	1.418(5)	1.443(3)	1.468(6)	1.426(3)	1.442(4)
C(25)−C(32)			1.431(6)		
C(26)−C(27)		1.427(3)	1.382(7)		1.418(4)
C(26)−C(31)			1.427(6)		
C(27)−C(28)		1.438(3)	1.395(8)		1.429(4)
C(28)−C(29)			1.380(8)		
C(29)−C(30)			1.419(7)		
C(30)−C(31)			1.422(7)		
C(1)···C(5) ring:					
av C−C	1.412(6)	1.420(4)	1.40(2)	1.40(7)	1.408(6)
C(6)···C(10) ring:					
av C−C	1.426(6)	1.430(9)	1.406(16)	1.418(9)	1.422(13)
Fe−C(1···5) av	2.039(7)	2.055(2)	2.023(13)	2.01(4)	2.034(5)
Fe−C(6···10) av	2.043(8)	2.056(6)	2.026(11)	2.041(7)	2.041(3)
C(10)−C(11)−C(12)	178.2(4)	178.7(3)	178.7(7)	126.42(18)	126.4(3)
C(11)−C(12)−C(13)	179.1(4)	175.3(3)	177.1(7)	123.28(18)	126.5(3)

Table 3. Orientation of the Rings Data

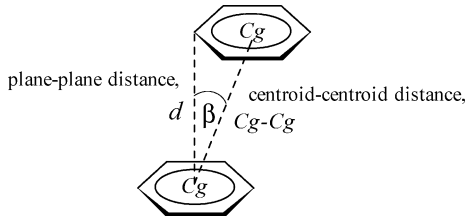

	displacement parameters for π-stacked aromatic rings[a]				
compd	α/deg[b]	β/deg[c]	*d*/Å[d]	*Cg*−*Cg*/Å[e]	*N*[f]
5	2.34	27.17	3.585	4.029	2
6	1.89−3.26	27.08−29.48	3.393−3.447	3.897−3.898	8
7	0.00−2.25	19.54−24.67	3.385−3.425	3.615−3.771	10
12	3.85	28.70	3.634	4.143	2
13	1.43−2.68	54.85−59.19	3.020−3.151	5.474−5.902	4

[a] Data from PLATON.[30] [b] Dihedral angle between stacked ring planes. [c] Angle(s) between the ring centroid vector and the ring normal to the plane(s) of one of the aromatic PAH rings. This defines the degree of displacement between the stacked rings. [d] Perpendicular distance between the planes of the stacked rings. [e] Centroid−centroid vector length between stacked aromatic rings. [f] Number of aromatic rings in the PAH moiety involved in significant off-set π-stacking interactions.

of the anthracene residue. In the solid-state structure the best fit planes of the anthracene and substituted cyclopentadienyl rings are found to subtend an angle of 83.89(5)° to one another, with an angle of 62.58(14)° between the anthracene and alkene [C(10)···C(13)] planes. A second minimization with the substituted cyclopentadienyl ring constrained to lie in the anthracene plane afforded a structure 25.98 kJ/mol higher in energy. The solid-state and calculated structures for the ethenylpyrene derivative **13** are also reasonably congruent but with a markedly different orientation of the cyclopentadienyl and polyaromatic rings compared to **12**. Here the free global minimum was found with the substituted cyclopentadienyl ring almost *coplanar* with the pyrene ring. This compares with the solid-state structure, where the corresponding angle is 33.93(13)° with an angle of 35.6(3)° between the pyrene and alkene [C(10)···C(13)] planes.

Given the small energy differences between the calculated orthogonal and coplanar orientations of the cyclopentadienyl and polyaromatic rings in most molecules, it is likely that these orientations and molecular packing are determined by optimization of offset π-stacking interactions[29] in the solid state. This appears to be the case with the probable exception of **13**. Representative views of typical π-stacking motifs are shown in Figure 4a−c, with details of the parallel displacement interactions shown in Table 3; all packing motifs are given in the Supporting Information.

(29) Janiak, C. *J. Chem. Soc., Dalton Trans.* **2000**, 3885.

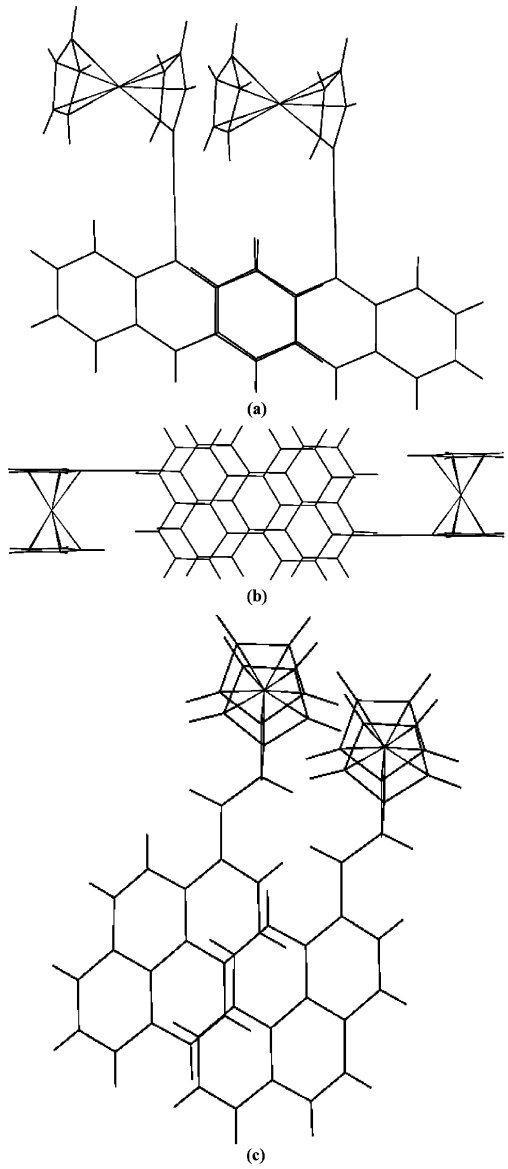

Figure 4. π-Stacking motifs for (a) **5**, symmetry relation between the two molecules $1+x, y, z$; (b) **7**, $2-x, -y, -z$; and (c) **13**, $x, y-1, z$.

These data reveal considerable similarities between the π-interactions between the anthracene rings in **5** and **12** and between the pyrene and perylene moieties of **6** and **7**. In both cases this is limited to interactions between pairs of molecules rather than extending throughout the structure. In the alkyne dyads **6** ad **7** (see for example Figure 4b), the orthogonal placement of the ferrocene moieties with respect to the polyaromatic rings facilitates stacking between pairs of molecules related by a pseudo C_2 axis; this effectively optimizes interactions between all of the aromatic rings of the pyrene and perylene systems (Table 3). In contrast, the degree of offset π-stacking between the pyrene rings of **13**, while again limited to pairs of molecules, is significantly less than is observed for the related alkyne derivative, with large displacement angles and inter-centroid distances (Figure 4c, Table 3). This suggests that offset π-stacking plays little part in stabilizing the solid-state structure in this case and strengthens the view that the trend toward orthogonal disposition of the cyclopentadienyl and polycyclic rings

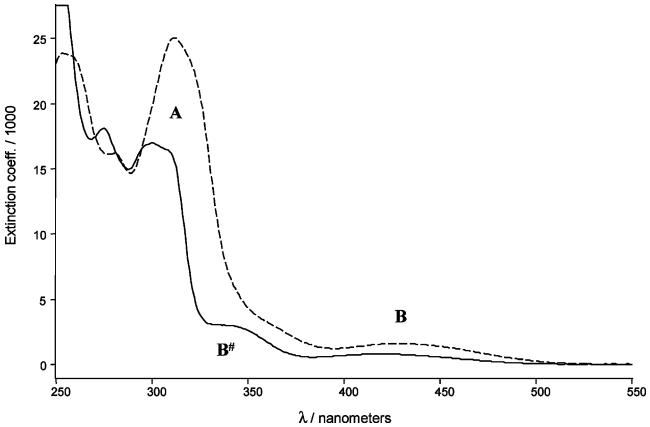

Figure 5. Electronic spectra in CH_2Cl_2, Fc−C≡C−(2)-naphthyl, **3** (—), Fc−CH=CH−(2)-naphthyl, **10** (- - -). Band **B#** is the second ferrocenyl d−d transition and is only discernible for compounds **1**−**4** and **8**.

for **5**−**7** may be largely determined by such packing effects. The exception to this argument is **12**. Simple steric considerations as well as the calculations described above point to the presence of strong nonbonding interactions between the alkene H on C_2 and the 1- and 8-H atoms of the anthryl group, which destabilize the all-planar situation by ca. 25.98 kJ/mol. It is also interesting to note however that, in the previously reported structure[8] of a TCNQ complex of **13**, strong offset π-stacking occurs between the pyrene rings and TCNQ molecules in interleaving stacks, with the inclination between the pyrene and substituted cyclopentadienyl rings reduced to 16.9°.

Spectroscopy of Neutral Dyads. The electronic spectra of the neutral dyads **1**−**18** between 300 and 1300 nm show two groups of absorption bands (Figure 5). **A** are the more intense (ϵ > 9000), lie between 300 and 450 nm, and have wavelengths which increase with increasing annelation of the Ar group. **B** are weaker (ϵ < 4000), lie between 440 and 460 nm, and have wavelengths that do not vary greatly with Ar (Table 1).

Absorption bands in the electronic spectra of the parent arenes are divided into the shorter β bands (ϵ = ca. 10^4−10^6) and the longer wavelength, substituent-sensitive p bands (ϵ = ca. 10^4), which become red-shifted with increasing annelation.[31] Bands **A** are assigned to the p bands of the Ar end-groups. The large red shifts of **A** compared with their ArH or Ar−C≡C−H counterparts are due to the Fc−C≡C group acting as a donor; this raises the energy of the Ar HOMO (confirmed by B3LYP calculations) and lowers the energy of its π−π^* transition. Vibrational fine structure similar to that found in the parent arene is visible in band **A** of the alkyne dyads. It has been observed recently[32] that ethynyl substitution of a PAH causes an average bathochromic shift of 18 nm in the wavelength of its p band with retention (but broadening) of its vibrational fine structure. As it is known that this vibrational fine structure is reduced when the aromatic residue is engaged in more extensive conjugation, this suggests

(30) Spek, A. L. *J. Appl. Crystallogr.* **2003**, *36*, 7.
(31) (a) Clar, E. *Polycyclic Hydrocarbons*, Vol. 1; Academic Press: London, 1964. (b) Jones, R. N. *Chem. Rev.* **1947**, *41*, 353.
(32) Marsh, N. D.; Mikolajczak, C. J.; Wornat, M. J. *Spectrochim. Acta Part A* **2000**, *56*, 1499.

that conjugation of the Ar and FcC≡C π-systems is not important in our dyads. With the ethenyl dyads, however, the absorption bands **A** are, in most cases, broad and featureless and at lower energies than their ethynyl counterparts. This suggests that the ferrocenyl group perturbs the arene π-orbitals where there is ethenyl, but not ethynyl, connectivity between the ferrocenyl and arene components. The poorer conjugation through an alkyne connection has been noted in other ferrocenyl systems.[3] Yet again, **12** is anomalous in that band **A** for **12** is higher in energy than for the equivalent band in **5** and displays vibrational fine structure. This implies the absence of ferrocenyl−anthryl electronic interactions and is consistent with the inability of **12** to form a planar molecule as a consequence of intramolecular steric interactions (see above).

The energy of **B**—446 nm for the ethyne series and 457 nm for the ethene series—is invariant with Ar and solvent and tracks closely those for Fc−C≡C−Fc (452 nm, $\epsilon = 820$) and Fc−CH=CH−Fc (458 nm, $\epsilon = 1450$)[33] and Fc−(CH=CH)$_2$−Fc at 466 nm ($\epsilon = 2800$).[10] Two weak metal-centered d−d bands at 325 and 440 nm characterize ferrocene and ferrocenyl compounds where the substituents are not strong acceptors or involved in conjugation.[3,34] **B** is therefore assigned to the low-energy ferrocenyl transition; it is obscured by the $\pi-\pi^*$ transition in the perylenyl dyads. This conclusion is reinforced by the resonance Raman spectra. For example, the resonance Raman spectrum of **5** ($\lambda_{exc} = 457.9$ nm) mirrors that of Fc−C≡CH, with enhancement of the $\nu_{C\equiv C}$ band at 2202 cm^{-1} and of the ferrocenyl bands at 1100 and 298 cm^{-1}, but no enhancement of the anthracene vibrational modes. This assignment is supported by B3LYP calculations, and a detailed analysis will be given in a subsequent paper.[16] If there was significant conjugation, the aryl orbitals would mix with the ferrocenylmetal d orbitals so the lowest energy band in the dyads would be a metal to ligand charge transition. The above data therefore show that the ferrocenyl group is the donor and that there is little communication between the two end-groups of the dyads.

Spectroelectrochemical Properties. Compounds **1**−**18** display the expected one-electron chemically reversible Fc$^+$/Fc^0 couple in cyclic voltammetric scans. The potential is dependent on the type of unsaturated link (Table 1) and is almost independent of Ar. For the ethynyl dyads E[Fc]$^{+/0}$ is 0.67−0.68 V in CH_2Cl_2 (all potentials vs [FeCp*$_2$]$^{+/0}$) and for most ethenyl dyads 0.55 ± 0.01 V. These potentials are similar to those for Fc−C≡C−H (0.72 V) or Fc−CH=CH$_2$ (0.56 V) and other ethenyl/ethynyl ferrocenyl systems with donor substituents.[2a,4,13,25,35] Ethenylferrocenes with electron-withdrawing groups have higher potentials; for example, E[Fc]$^{+/0}$ = ∼0.58 and 0.60 V for Fc−CH=CH-p-NO$_2$-phenyl[2a] and Fc−CH=CH-naphthalimide,[15] respectively. Again, **12** is anomalous, being more difficult to oxidize than other ethenyl dyads. Attempts to isolate the chemically generated cations were unsuccessful. Cyclic voltammetry also shows complex reduction processes on the cathodic scans of all dyads associated with the formation of radical anions; these correspond to those found in the electrochemistry of the parent arene. Parameters from the ESR spectra of the radical anions generated electrochemically at 213 K (see Experimental Section) are identical to those of the respective arene radical anion, which locates the LUMO for the dyads on the aromatic component. The electrochemical data support the view that the ferrocenyl and arene components function as independent entities in these dyads.

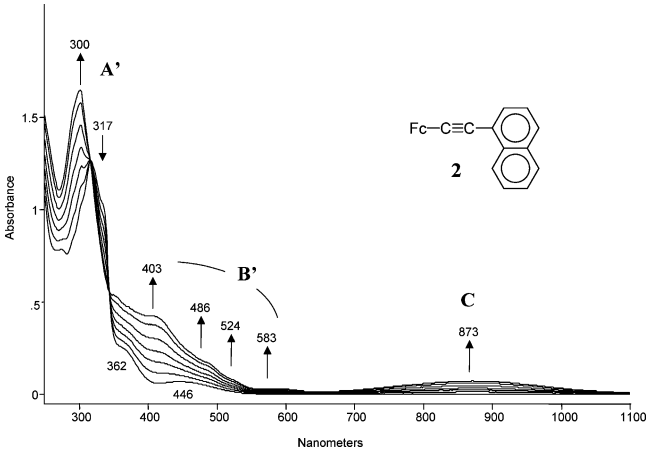

Figure 6. UV−vis OTTLE spectra of **2** (0−0.7 V, CH_2Cl_2).

OTTLE vibrational and electronic spectra show consistent isosbestic points and complete reversibility when the potential is cycled (0.0−0.7 V), attesting to the stability of the monocations **1**$^+$−**18**$^+$. Representation of these cations as {Fc$^+$}−C≡C−{aryl} in the ground state is indicated by the vibrational data. Although the aryl vibrational modes are unaffected by oxidation, the Fc-based vibrational bands shift in the same way as those of ferrocene upon oxidation. For example, the resonance Raman spectrum of **5**$^+$ shows a shift of the Fc ring-breathing mode of +7 cm^{-1}, and there is a typical Fc$^+$ band at 1113 cm^{-1} in the infrared spectrum.

Significant changes occur in the electronic spectra upon oxidation (Figure 6). Band **A** undergoes a small blue shift, as the Fc−(π-link) is a much weaker donor in the oxidized species. If we follow the dictum enunciated above that the vibrational structure on the $\pi\pi^*$ transition reflects the relative ring orientations, then the orthogonal structure is retained in all of the ethyne ferrocenium derivatives. Likewise, there appears to be no change in the ring orientation for the ethenyl analogues upon oxidation; the anthryl derivative is still anomalous. Band **B** in the neutral dyad is replaced by a complex structured feature, **B′**, covering a wide energy range, and **B″** at lower energy and very weak intensity. Unlike **B** however, the structure and energy of these two bands are dependent on the aryl group and solvent, but still essentially independent of the type of π-link (Table 1). An important observation is that the resonance Raman spectra resonant with band **B′** ($\lambda_{exc} = 457.9$ nm) show an enhancement of modes associated with both the arene and Fc$^+$ units. Furthermore, Fc/Fc$^+$ ring-breathing modes show an increased resonance enhancement on going to the monocations, whereas there is a 3-fold decrease in enhancement in the equivalent modes for FcH to FcH$^+$. These data imply that the Fc-based modes are deriving enhancement from an additional electronic transition that is not isolated on the metallocene. This substantiates a charge transfer

(33) Rosenblum, M.; Brawn, N.; Papenmeier, J.; Applebaum, M. *J. Organomet. Chem.* **1966**, *6*, 173.
(34) Sohn, Y. S.; Hendrickson, D. N.; Gray, H. B. *J. Am. Chem. Soc.* **1971**, *93*, 3603.

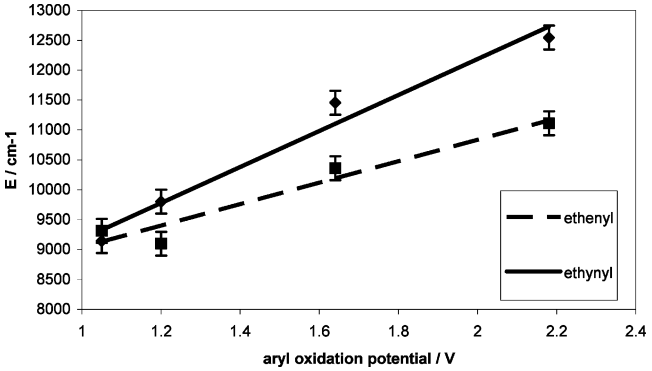

Figure 7. Correlation of band **C** energy against aryl oxidation potential; CH_2Cl_2; potential in volts.

assignment for **B′** with the excited state having both ferrocenyl and arene character. The most striking new features are the low intensity, charge transfer bands **C** (Figure 5b, Table 1). Bands **C** are assigned to the LMCT transitions, $Fc^+ \leftarrow \{C{\equiv}C{-}Ar\}$. This LMCT assignment is supported by the following observations: first, dependence of the energy of **C** on the aryl end-group (Table 1); second, a large negative solvatochromic shift of 1000−1500 cm^{-1} on going from CH_2Cl_2 to MeCN, supportive of a larger dipole in the ground state than the excited state; third, the trend in the energies of **C** should correlate with the difference in energy between the donor and acceptor orbitals. Given that the energy of the acceptor orbital, approximated by the $[Fc]^{+/0}$ reduction potential, is constant for a specific π-link, these energies should correlate with energy of the donor aryl orbital. Plots of the electrochemical oxidation potentials or ionization energies of the respective aryl versus the energy of band **C** are indeed linear (Figure 7); the ethene energies are red-shifted relative to their ethyne counterparts except for the anthryl dyads. Finally, there is an enhancement of both arene and Fc^+ vibrational modes in the resonance Raman spectrum of the monocations. Bands similar to **C** have been observed[4,11,36] for many arrays where donor end-groups have been connected to a ferrocenium moiety via an unsaturated link, and a detailed spectroscopic analysis and theoretical calculations of these LMCT transitions will be given in another paper.[16]

Conclusion

This sequence of ferrocenyl−aryl dyads with ethenyl and ethynyl π-linkages has given an additional insight into the structural and spectral parameters that would impact on their incorporation in NLO and fluorophore materials. The Fc−C═C− or Fc−C≡C− component acts as the donor in the ground state, and there is no communication between the ferrocenyl and aryl end-groups. Subtle packing effects and π-stacking determine the orientation of the Cp(Fc) ring relative to the arene ring plane in the solid state; the rings are essentially coplanar in the ethenyl and orthogonal in the ethynyl dyads. Given the importance of intermolecular interactions, it should be possible to freeze specific ring plane orientations with the appropriate choice of ring substituents. With the exception of the ethenylanthryl dyad, there are only small variations in physical properties with the aryl end-group for a particular π-linkage. Why the spectroscopic and redox properties of **12** and $\mathbf{12}^+$ in solution, as well the solid-state structure of **12**, are so different is a puzzle, unless the strong nonbonding interactions that are a feature of this dyad cause a significant perturbation of the electronic structure. Calculations do not support this premise however.

Oxidation of the dyads at the ferrocenyl end-group creates a situation where the relative energies and overlap of ferrocenium and aryl orbitals stimulate a classical donor−acceptor interaction that does not occur in the neutral precursors. The energy of the resulting weak LMCT transition in the NIR can be predicted for the ionization energy of the aryl end-group. Furthermore, the absorption of NIR radiation can be switched on or off via the ferrocenyl couple, an electrochromic system.[37] The challenge is to increase, by an order of magnitude, the extinction coefficient of the NIR absorption so that the materials have technological significance.

Experimental Section

Solvents were dried and distilled by standard procedures, and all reactions unless stated were performed under nitrogen. Microanalyses were carried out by the Campbell Microanalytical Laboratory, University of Otago. Melting points were recorded on an Electrothermal digital melting point apparatus and are uncorrected. Mass spectra were recorded on a Kratos MS80RFA instrument with an Iontech ZN11NF atom gun. IR spectra were recorded on a Perkin-Elmer Spectrum BX FT-IR spectrometer, ^1H and ^{13}C NMR spectra on Varian Unity Inova 300 and 500 MHz spectrometers in $CDCl_3$ (7.26 ppm) at 25 °C, and electronic spectra on a Varian Cary 500 UV−vis spectrophotometer. Cyclic and square-wave voltammetry in CH_2Cl_2 were performed using a three-electrode cell with a polished Pt 1 mm disk working electrode; solutions were $\sim 10^{-3}$ M in electroactive material and 0.10 M in supporting electrolyte (recrystallized $TBAPF_6$). Data were recorded on an EG & G PAR 273A or Powerlab/4sp computer-controlled potentiostat. Scan rates of 0.05−1 V s^{-1} were typically employed for cyclic voltammetry and for square-wave voltammetry, square-wave step heights of 5 mV and a square amplitude of 25 mV with a frequency of 15 Hz. All potentials are referenced to decamethylferrocene; $E_{1/2}$ for sublimed ferrocene was 0.55 V. Infrared and UV−vis OTTLE data were obtained from standard cells with platinum grid electrodes. ESR spectra were obtained using a Bruker EMX X-band spectrometer equipped with a Bruker variable-temperature accessory, a Systron-Donner microwave frequency counter, and a Bruker gaussmeter; ca. 5 mM THF/$TBAPF_6$ solutions of the compound were reduced electrochemically in situ. The B3LYP method was used for all calculations with a 6-31G(D) basis set; the program was the G98 revision A7[i], and where geometries were constrained, this was done using the ADDREDUNDANT key word after which the appropriate dihedral angles were set. Molec-

(35) (a) Fink, H.; Long, N. J.; Martin, A. J.; Opromolla, G.; White, A. J. P.; Williams, D. J.; Zanello, P. *Organometallics* **1997**, *16*, 2646. (b) Jones, N. D.; Wolf, M. O.; Giaquinta, D. M. *Organometallics* **1997**, *16*, 1352. (c) Sato, M.; Shintate, H.; Kawata, Y.; Sekino, M.; Katada, M.; Kawata, S. *Organometallics* **1994**, *13*, 1956. (d) Osella, D.; Gambino, O.; Nervi, C.; Ravera, M.; Vittoria Russo, M.; Infante, G. *Inorg Chim. Acta* **1994**, *225*, 35. (e) Wong, W.-Y.; Lu, G.-L.; Ng, K.-F.; Wong, C.-K.; Choi, K.-H. *J. Organomet. Chem.* **2001**, *637−639*, 159. (f) Siemeling, U.; Vorfield, U.; Neumann, B.; Stammler, H.-G.; Zanello, P.; Fabrizi de Biani, F. *Eur. J. Inorg. Chem.* **1999**, 1. (g) Hsung, R. P.; Chidsey, C. E. D.; Sita, L. R. *Organometallics* **1995**, *14*, 4808.

(36) Toma, S.; Gaplovsky, A.; Hudecek, M.; Langfelderova, Z. *Monatsh. Chem.* **1985**, *116*, 357.

(37) Ward, M. D.; McCleverty, J. A. *J. Chem. Soc., Dalton Trans.* **2002**, 275.

ular orbital contour plots were prepared by importing the Gaussian 98 output files into MOLDEN. Formylvinylferrocene,[22] ferrocenylmethyl(triphenyl)phosphonium iodide,[38] and 3-iodoperylene[39] were prepared according to literature procedures. Other compounds were commercial reagents, used as received. Although syntheses of **10**, **13**, and **15** have been previously described,[8,19−21] ^{1}H NMR and IR data were not included and are thus included here for completeness.

Synthesis of Ethynyl Dyads. (9-Anthryl)ethynylferrocene (5). A typical preparation, that of **5**, follows. Ethynylferrocene (0.252 g, 1.2 mmol), 9-bromoanthracene (0.206 g, 0.8 mmol), and catalytic amounts (0.2 mol %) of $PdCl_2(PPh_3)_2$ and CuI were refluxed in 10 mL of $^iPr_2NH$ for 30 min. Solvent was removed under vacuum and the reaction mixture separated using chromatography on SiO_2 with a hexane/CH_2Cl_2 (3:1) eluant to give orange crystals of **5** (0.141 g, 46%), mp 218−220 °C. Anal. Calcd for $C_{26}H_{18}Fe$: C, 80.85; H, 4.70. Found: C, 80.84; H, 4.68. MS: *m/e* 386 (M^+). ^{1}H NMR (δ): 4.34 (s, 5H, C_5H_5), 4.36 (t, 2H, Fc-H_β), 4.72 (t, 2H, Fc-H_α), 7.52 (m, 2H, anthr-*H3/6*), 7.61 (m, 2H, anthr-*H2/7*), 8.02 (m, 2H, anthr-*H4/5*), 8.42 (s, anthr-*H10*), 8.61 (m, 2H, anthr-*H1/8*). IR (CH_2Cl_2): $\nu_{C\equiv C}$ 2203 cm^{-1}.

(2-Naphthyl)ethynylferrocene (3). From ethynylferrocene/2-bromonaphthalene; orange crystals (59%), mp 135 °C. Anal. Calcd for $C_{22}H_{16}Fe$: C, 78.59; H, 4.80. Found: C, 78.34; H, 4.88. MS: *m/e* 337 (MH^+). ^{1}H NMR (δ): 4.28 (s, 5H, C_5H_5), 4.27 (t, 2H, Fc-H_β), 4.55 (t, 2H, Fc-H_α), 7.49 (m, 2H, naphth-*H6*, *H7*), 7.55 [dd (J = 8, 2 Hz), naphth-*H3*], 7.79 (m, naphth-*H4*), 7.82 (m, 2H, naphth-*H5*, *H8*), 8.01 (m, naphth-*H1*). IR (CH_2Cl_2): $\nu_{C\equiv C}$ 2221, 2210 cm^{-1}.

(9-Phenanthryl)ethynylferrocene (4). From ethynylferrocene/9-bromophenanthrene; red-orange oil (30%). MS: *m/e* 387 (MH^+). ^{1}H NMR (δ): 4.32 (s, 5H, C_5H_5), 4.32 (t, 2H, Fc-H_β), 4.65 (t, 2H, Fc-H_α), 7.60 (m, phen-*H2*), 7.66 (m, phen-*H3*), 7.72 (m, 2H, phen-*H6*, *H7*), 7.87 (m, phen-*H1*), 8.04 (s, phen-*H10*), 8.52 (m, phen-*H8*), 8.67 (m, phen-*H4*), 8.71 (m, phen-*H5*). IR (CH_2Cl_2): $\nu_{C\equiv C}$ 2209 cm^{-1}.

(1-Pyrenyl)ethynylferrocene (6). From ethynylferrocene/1-iodopyrene; red-orange crystals (37%), mp 212−214 °C. Anal. Calcd for $C_{28}H_{18}Fe$: C, 81.97; H, 4.42. Found: C, 82.00; H, 4.41. MS: *m/e* 411 (MH^+). ^{1}H NMR (δ): 4.34 (s, 5H, C_5H_5), 4.34 (t, 2H, Fc-H_β), 4.68 (t, 2H, Fc-H_α), 8.03 [t (J = 8 Hz), pyr-*H7*], 8.05, 8.09 {2 × [d (J = 9 Hz)] pyr-*H4*, *H5*}, 8.12, 8.17 {2 × [d (J = 8 Hz)], pyr-*H3*, *H2*}, 8.20 (m, 2H, pyr-*H6*, *H9*), 8.23 [d (J = 8 Hz), pyr-*H8*], 8.63 [d (J = 9 Hz), pyr-*H10*]. IR (CH_2Cl_2): $\nu_{C\equiv C}$ 2221, 2202 cm^{-1}.

(3-Perylenyl)ethynylferrocene (7). From ethynylferrocene/3-iodoperylene; red-orange crystals (19%), mp >220 °C (with dec). Anal. Calcd for $C_{32}H_{20}Fe$: C, 83.49; H, 4.38. Found: C, 83.24; H, 4.63. MS: *m/e* 460 (M^+). ^{1}H NMR (δ): 4.31 (s, 5H, C_5H_5), 4.32 (t, 2H, Fc-H_β), 4.63 (t, 2H, Fc-H_α), 7.50 (m, 2H, per-*H8*, *H11*), 7.61 (m, per-*H5*), 7.70 (m, 3H, per-*H2*, *H9*, *H10*), 8.15 (m, per-*H1*), 8.20, 8.23 [2 × (m), per-*H7*, *H12*], 8.26 (m, per-*H6*), 8.27 (m, per-*H4*). IR (CH_2Cl_2): $\nu_{C\equiv C}$ 2207 cm^{-1}.

Synthesis of Ethenyl Dyads. (*E*)-(1-Naphthyl)ethenylferrocene (9). 1-Naphthaldehyde (0.630 g, 4.0 mmol) was dissolved in THF (50 mL), and ferrocenylmethyl triphenylphosphonium iodide (0.966 g, 2.0 mmol) was added. Solid KO^{t}Bu (0.224 g, 2.0 mmol) was introduced in one portion, and the mixture was stirred at room temperature for 2 h. The reaction was quenched with water (100 mL), extracted with diethyl ether (100 mL), washed with water, and dried over $MgSO_4$. Concentration in vacuo afforded an orange solid. This was redissolved in dichloromethane (10 mL) and heated at reflux with a crystal of iodine until TLC indicated the presence of only one isomer. The solution was washed with aqueous thiosulfate solution (10 mL) and water followed by extraction, drying, and removal of the solvent as before. The solid residue was purified by column chromatography on silica gel with hexane/CH_2Cl_2 (4:1) eluant, and the product was crystallized from CH_2Cl_2/hexane to give orange crystals (0.155 g, 23%), mp 125−128 °C. Anal. Calcd for $C_{22}H_{18}Fe$: C, 78.11; H, 5.33. Found: C, 78.09; H, 5.44. MS: *m/e* 339 (MH^+). ^{1}H NMR (δ): 4.19 (s, 5H, C_5H_5), 4.33 (t, 2H, Fc-H_β), 4.56 (t, 2H, Fc-H_α), 6.93 [d (J = 16 Hz), Fc-C*H*=], 7.48 [d (J = 16 Hz), =C*H*-naphth], 7.49 (m, naphth-*H3*), 7.5 (m, 2H, naphth-*H6*, *H7*), 7.70 (m, naphth-*H2*), 7.78 (m, naphth-*H4*) 7.87 (m, naphth-*H5*), 8.19 (m, naphth-*H8*). IR (CH_2Cl_2): 950 (*E*-CH=CH wag) cm^{-1}.

(*E*)-(2-Naphthyl)ethenylferrocene (10). From $FcCH_2PPh_3^+I^-$/2-naphthaldehyde; orange crystals (46%), mp 165−167 °C. Anal. Calcd for $C_{22}H_{18}Fe$: C, 78.11; H, 5.33. Found: C, 78.05; H, 5.32. MS: *m/e* 339 (MH^+). ^{1}H NMR (δ): 4.16 (s, 5H, C_5H_5), 4.31 (t, 2H, Fc-H_β), 4.52 (t, 2H, Fc-H_α), 6.87 [d (J = 16 Hz), =C*H*-naphth], 7.01 [d (J = 16 Hz), Fc-C*H*=], 7.45 (m, 2H, naphth-*H6*, *H7*), 7.68 [dd (J = 9, 2 Hz), naphth-*H3*], 7.76 (m, naphth-*H1*), 7.8 (m, 3H, naphth-*H4*, *H5*, *H8*). IR (CH_2Cl_2): 959 (*E*-CH=CH wag) cm^{-1}.

(*E*)-(9-Phenanthryl)ethenylferrocene (11). From $FcCH_2PPh_3^+I^-$/9-phenanthrenecarboxaldehyde; orange red crystals (51%), mp 133−135 °C. Anal. Calcd for $C_{26}H_{20}Fe$: C, 80.41; H, 5.15. Found: C, 80.13; H, 5.23. MS: *m/e* 389 (MH^+). ^{1}H NMR (δ): 4.22 (s, 5H, C_5H_5), 4.35 (t, 2H, Fc-H_β), 4.59 (t, 2H, Fc-H_α), 7.01 [d (J = 16 Hz), Fc-C*H*=], 7.47 [d (J = 16 Hz), =C*H*-phen], 7.6 (m, 4H, phen-*H2*, *H3*, *H6*, *H7*), 7.91 (s, phen-*H10*), 7.92 (m, phen-*H1*), 8.24 (m, phen-*H8*), 8.67 (m, phen-*H4*), 8.75 (m, phen-*H5*). IR (CH_2Cl_2): 958 (*E*-CH=CH wag) cm^{-1}.

(*E*)-(9-Anthryl)ethenylferrocene (12). From $FcCH_2PPh_3^+I^-$/9-anthraldehyde; orange crystals (36%), mp 177−178 °C. Anal. Calcd for $C_{26}H_{20}Fe$: C, 80.41; H, 5.15. Found: C, 80.23; H, 5.45. MS: *m/e* 389 (MH^+). ^{1}H NMR (δ): 4.29 (s, 5H, C_5H_5), 4.38 (t, 2H, Fc-H_β), 4.63 (t, 2H, Fc-H_α), 6.71 [d (J = 16 Hz), Fc-C*H*=], 7.48 (m, 4H, anthr-*H2/7*, *H3/6*), 7.51 [d (J = 16 Hz), =C*H*-anthr], 8.02 (m, 2H, anthr-*H4/5*), 8.39 (s, anthr-*H10*), 8.40 (m, 2H, anthr-*H1/8*). IR (CH_2Cl_2): 958 (*E*-CH=CH wag) cm^{-1}.

(*E*)-(1-Pyrenyl)ethenylferrocene (13). From $FcCH_2PPh_3^+I^-$/1-pyrenecarboxaldehyde; red crystals (46%), mp 190−191 °C. Anal. Calcd for $C_{28}H_{20}Fe$: C, 81.55; H, 4.85. Found: C, 81.43; H, 5.00. MS: *m/e* 413 (MH^+). ^{1}H NMR (δ): 4.22 (s, 5H, C_5H_5), 4.34 (t, 2H, Fc-H_β), 4.64 (t, 2H, Fc-H_α), 7.14 [d (J = 16 Hz), Fc-C*H*=], 7.78 [d (J = 16 Hz), =C*H*-pyr], 8.00 [t (J = 8 Hz), pyr-*H7*], 8.05 (s, 2H, pyr-*H4*, *H5*), 8.13 [d (J = 9 Hz), pyr-*H9*], 8.16 [d (J = 8 Hz), pyr-*H3*], 8.18 [d (J = 8 Hz), 2H, pyr-*H6*, *H8*], 8.27 [d (J = 8 Hz), pyr-*H2*], 8.45 [d (J = 9 Hz), pyr-*H10*]. IR (CH_2Cl_2): 956 (*E*-CH=CH wag) cm^{-1}.

(*E*)-(3-perylenyl)ethenylferrocene (14). From $FcCH_2PPh_3^+I^-$/3-perylenecarboxaldehyde; red crystals (74%), mp 170 °C. Anal. Calcd for $C_{32}H_{22}Fe$: C, 83.13; H, 4.80. Found: C, 83.32; H, 4.68. MS: *m/e* 462 (M^+). ^{1}H NMR (δ): 4.20 (s, 5H, C_5H_5), 4.35 (t, 2H, Fc-H_β), 4.58 (t, 2H, Fc-H_α), 6.98 [d (J = 16 Hz), Fc-C*H*=], 7.41 [d (J = 16 Hz), =C*H*-per], 7.49 (m, 2H, per-*H8*, *H11*), 7.55 (m, per-*H5*), 7.68, 7.69 [2 × (m), per-*H9*, *H10*], 7.72 [d (J = 8 Hz), per-*H2*], 8.04 (m, per-*H4*), 8.19 [d (J = 8 Hz), per-*H1*], 8.19, 8.21 [2 × (m), per-*H7*, *H12*], 8.24 (m, per-*H6*). IR (CH_2Cl_2): 956 (*E*-CH=CH wag) cm^{-1}.

Synthesis of Butadienyl Dyads. (*E*,*E*)-(Phenyl)butadienylferrocene (15). ^{t}BuOK (0.033 g, 0.2 mmol) was added to a solution of $[PhCH_2PPh_3]Br$ (0.106 g, 0.2 mmol) in dry ether (25 mL). After 30 min, FcCH=CHCHO (0.048 g, 0.19 mmol) was added to the solution and the mixture stirred overnight. It was quenched with water (25 mL) and the organic layer washed with more water, dried over magnesium sulfate, and evaporated to dryness to give an orange solid. This was redissolved in dichloromethane (10 mL) and heated at reflux with a crystal of iodine until TLC indicated the presence of only one isomer. The solution was washed with aqueous

(38) Baumgarten, H. E., Ed. *Organic Syntheses*; Wiley: New York, 1973; Collect. Vol. V, p 434.
(39) Inouye, M.; Hyodo, Y.; Nakazumi, H. *J. Org. Chem.* **1999**, *64*, 2704.

Table 4. Crystal Data

	5	6	7	12	13
chem formula	$C_{26}H_{18}Fe$	$C_{28}H_{18}Fe$	$C_{32}H_{20}Fe$	$C_{26}H_{20}Fe$	$C_{28}H_{20}Fe$
fw	386.25	410.27	460.33	388.27	412.29
cryst syst	monoclinic	triclinic	monoclinic	triclinic	monoclinic
space group	$P2_1/c$	$P\bar{1}$	$P2_1/c$	$P\bar{1}$	$P2_1/c$
absorp coeff/mm^{-1}	0.849	0.826	0.735	0.812	0.778
final R indices [$I>2\sigma(I)$]	R1 = 0.0423	R1 = 0.0374	R1 = 0.0754	R1 = 0.0345	R1 = 0.0363
	wR2 = 0.1010	wR2 = 0.0894	wR2 = 0.2192	wR2 = 0.1033	wR2 = 0.0594
R indices (all data)	R1 = 0.0608	R1 = 0.0515	R1 = 0.0891	R1 = 0.0436	R1 = 0.1020
	wR2 = 0.1075	wR2 = 0.0930	wR2 = 0.2279	wR2 = 0.0905	wR2 = 0.0696
unit cell dimens					
a/Å	7.265(3)	7.810(5)	11.4212(10)	7.7278(4)	19.12(3)
b/Å	11.059(4)	9.956(6)	10.8680(10)	10.5188(9)	7.379(9)
c/Å	22.303(8)	13.205(8)	17.2066(16)	12.0885(8)	14.89(3)
α/deg	90	107.540(6)	90	101.449(5)	90
β/deg	91.824(5)	101.733(7)	99.6090(10)	100.901(4)	110.62(3)
γ/deg	90	100.521(6)	90	95.453(5)	90
volume/Å^3	1791.2(10)	925.4(10)	2105.8(3)	936.69(11)	1966(5)
Z	4	2	4	2	4
temp/K	168(2)	163(2)	158(2)	294(2)	168(2)
no. of reflns collected	3710	11 682	14 350	5507	23 370
no. of indep reflns	2421	3719	4127	4528	4001
	[R(int) = 0.0275]	[R(int) = 0.0463]	[R(int) = 0.0233]	[R(int) = 0.00142]	[R(int) = 0.0841]

sodium thiosulfate solution (10 mL) and water followed by extraction, drying, and removal of the solvent as before. The solid residue was purified by column chromatography on silica gel with hexane/CH_2Cl_2 (1:3) to give orange crystals (0.037 gm, 63%), mp 198−201°C. Anal. Calcd for $C_{20}H_{18}Fe$: C, 76.45; H, 5.77. Found: C, 76.33; H, 5.64. MS: *m/e* 315 (MH^+). ^{1}H NMR (δ): 4.13 (s, 5H, C_5H_5), 4.28 (t, 2H, Fc-H_β), 4.41 (t, 2H, Fc-H_α), 6.44 [d (J = 15 Hz), Fc-C*H*=], 6.54 [d (J = 15 Hz), =C*H*-naphth], 6.56 [dd (J = 10, 15 Hz), Fc-CH=C*H*], 6.85 [dd (J = 10, 15 Hz), C*H*=CH-naphth], 7.22 (m, phenyl-*H4*), 7.32 (m, 2H, phenyl-*H3/5*), 7.42 (m, 2H, phenyl-*H2/6*).

(*E,E*)-(2-Naphthyl)butadienylferrocene (16). From FcCH=CH−CHO/(2-naphthyl)-$CH_2PPh_3^+I^-$; orange crystals (36%), mp 203−204 °C. Anal. Calcd for $C_{24}H_{20}Fe$: C, 79.14; H, 5.53. Found: C, 79.34; H, 6.21. MS: *m/e* 365 (MH^+). ^{1}H NMR (δ): 4.15 (s, 5H, C_5H_5), 4.30 (t, 2H, Fc-H_β), 4.44 (t, 2H, Fc-H_α), 6.48 [d (J = 15 Hz), =C*H*-naphth], 6.62 [dd (J = 10, 15 Hz), C*H*=CH-naphth], 6.69 [d (J = 15 Hz), Fc-C*H*=], 6.98 [dd (J = 10, 15 Hz), Fc-CH=C*H*], 7.44 (m, 2H, naphth-*H6*, *H7*), 7.64 [dd (J = 9, 2 Hz), naphth-*H3*], 7.8 (m, 4H, naphth-*H1*,*4*,*5*,*8*).

(*E,E*)-(9-Anthryl)butadienylferrocene (17). From FcCH=CH−CHO/(9-anthryl)-$CH_2PPh_3^+I^-$; orange crystals (10%). Anal. Calcd for $C_{28}H_{22}Fe$: C, 81.17; H, 5.35. Found: C, 80.78; H, 5.56. MS: *m/e* 415 (MH^+). ^{1}H NMR (δ): 4.19 (s, 5H, C_5H_5), 4.38 (t, 2H, Fc-H_β), 4.63 (t, 2H, Fc-H_α), 6.48 [d (J = 15 Hz), Fc-C*H*=], 6.69 [dd (J = 10, 15 Hz), C*H*=CH-anthr], 6.85 [dd (J = 10, 15 Hz), Fc-CH=C*H*], 7.38 [d (J = 15 Hz), =C*H*-anthr], 7.48 (m, 4H, anthr-*H2/7*, *H3/6*), 8.01 (m, 2H, anthr-*H4/5*), 8.35 (m, 2H, anthr-*H1/8*), 8.38 (s, anthr-*H10*).

(*E,E*)-(1-Pyrenyl)butadienylferrocene (18). From FcCH=CH−CHO/(1-pyrenyl)-$CH_2PPh_3^+I^-$; orange crystals (20%). Anal. Calcd for $C_{30}H_{22}Fe$: C, 82.20; H, 5.06. Found: C, 82.12; H, 5.07. MS: *m/e* 439 (MH^+). ^{1}H NMR (δ): 4.19 (s, 5H, C_5H_5), 4.35 (t, 2H, Fc-H_β), 4.50 (t, 2H, Fc-H_α), 6.57 [d (J = 15 Hz), Fc-C*H*=], 6.80 [dd (J = 10, 15 Hz), Fc-CH=C*H*], 7.14 [dd (J = 10, 15 Hz), C*H*=CH-pyr], 7.62 [d (J = 15 Hz), =C*H*-pyr], 8.00 [t (J = 8 Hz), pyr-*H7*], 8.1 (m, 6H, pyr-*H3-6*,*8*,*9*), 8.28 [d (J = 8 Hz), pyr-*H2*], 8.46 [d, (J = 9 Hz), pyr-*H10*].

X-ray Data Collection, Reduction, and Structure Solution for 5−7, 12, and 13. Crystal data for compounds **5**−**7**, **12**, and **13** are given in Table 4. Data for **5**−**7** and **13** were collected at low temperatures on a Bruker SMART CCD diffractometer, processed using SAINT[40] with empirical absorption corrections applied using SADABS.[40] For **12**, data were obtained at 294(2) K on a Siemens P4 diffractometer. The absorption corrections were undertaken using ψ-scans and the program XEMP in XSCANS.[41]

All structures were solved by direct methods using SHELXS[42] and refined by full-matrix least-squares on F^2 using TITAN2000[43] and SHELXL-97.[42] Non-hydrogen atoms were assigned anisotropic temperature factors, with hydrogen atoms included in calculated positions. High and increasing temperature factors for the C1−C5 atoms of the unsubstituted cyclopentadienyl ring in **12** indicated that the ring was disordered over two sites. The disorder was resolved by refining two unique positions for these atoms with their occupancy factors f and f' refined such that $f' = 1 - f$. The final value of f refined to 0.568(16). The final difference Fourier synthesis for **13** revealed a high peak (~2 e Å^{-3}) close to the C20 atom of the perylene ring. This clearly contributes to the relatively high residuals observed in the refinement. However, no sensible chemical assignment of the peak could be made and there was no indication of it resulting from disorder.

Acknowledgment. We thank Prof. Ward T. Robinson and Dr. Jan Wikaira (University of Canterbury) for X-ray data collection, Dr. Amar Flood for the resonance Raman data, and Drs. Keith Gordon and Henrik Kjaergaard for helpful discussions.

Supporting Information Available: Final positional and equivalent thermal parameters are given in the deposited tables, all bond lengths and angles, anisotropic thermal parameters, and hydrogen positional and isotropic displacement parameters for all compounds. Calculated global minimized structures and packing motifs are given in Figures S1−S4. ^{1}H and ^{13}C NMR are given in Tables S1−S5 and Figures S5−S11. This material is available free of charge via the Internet at http://pubs.acs.org

OM0492653

(40) *SMART* (control) and *SAINT* (integration) software; Bruker AXS: Madison WI, 1994. *SADABS* (correction for area detector data); Bruker, 1997.

(41) *XEMP* absorption correction routine in XSCANS, Siemens, 1996.

(42) Sheldrick, G. M. *SHELXS*: a program for the solution of crystal structures from diffraction data, 1990; *SHELXL-97*: a program for the refinement of crystal structures, 1997; University of Göttingen, Germany.

(43) Hunter K. A.; Simpson J. *TITAN2000*: A molecular graphics program to aid structure solution and refinement with the SHELX suite of programs; University of Otago, New Zealand, 1999.